Measurement of the $\vec{d}\,\vec{p} \to \{pp\}\,n$ Charge–Exchange Reaction with Polarised Beam and Target

A. Garishvili, A. Kacharava, A. Nass, A. Mussgiller, E. Steffens
Physikalisches Institut II, Universität Erlangen–Nürnberg, 91058 Erlangen, Germany

V.V. Glagolev
Joint Institute for Nuclear Research, Laboratory of High Energy, 141980 Dubna, Russia

L. Barion, D. Chiladze, A. Dzyuba, R. Engels, R. Gebel, K. Grigoriev, M. Hartmann, V. Hejny, I. Keshelashvili, B. Lorentz, M. Mikirtytchiants, M. Nekipelov, D. Oellers, H. Ohm, D. Prasuhn, F. Rathmann, R. Schleichert, H. Seyfarth, H.J. Stein, H. Ströher, Yu. Valdau
Institut für Kernphysik, Forschungszentrum Jülich, 52425 Jülich, Germany

S. Dymov, D. Gusev, V. Komarov, A. Kulikov, V. Kurbatov, V. Leontiev, G. Macharashvili, S. Merzliakov, V. Serdjuk, S. Trusov, Yu. Uzikov
Joint Institute for Nuclear Research, LNP, 141980 Dubna, Russia

B. Chiladze, D. Iamanidze, N. Lomidze, M. Nioradze, M. Tabidze
High Energy Physics Institute, Tbilisi State University, 0186 Tbilisi, Georgia

A. Khoukaz, T. Mersmann, M. Mielke, M. Papenbrock, T. Rausmann
Institut für Kernphysik, Universität Münster, 48149 Münster, Germany

S. Barsov, V. Koptev, S. Mikirtytchiants, A. Vassiliev
High Energy Physics Department, Petersburg Nuclear Physics Institute, 188350 Gatchina, Russia

J. Carbonell
Laboratoire de Physique Subatomique et de Cosmologie, 38026 Grenoble Cedex, France

C. Wilkin
Physics and Astronomy Department, UCL, London WC1E 6BT, U.K.

for the ANKE Collaboration

Jülich, 29 September 2006

Abstract

Our study of the $\vec{d}p \to (pp)n$ deuteron charge–exchange reaction has shown that we can successfully investigate reactions with a polarised deuteron beam. In particular, we have proved that we can calibrate the vector and tensor polarisations of such a beam. Since the necessary equipment has already been installed, it is now time to advance our programme by proposing experiments using a polarised target cell in conjunction with a polarised beam.

At low excitation energies E_{pp} of the final pp system, the spin observables are directly related to the spin–dependent parts of the neutron–proton charge–exchange amplitudes. Our measurement of the deuteron–proton spin correlations will allow us to determine the relative phases of these amplitudes in addition to their overall magnitudes (which can be determined from the unpolarised cross section and deuteron tensor analysing powers). This is the primary aim of our present proposal.

Furthermore, the experiment is crucial in: (i) teaching us how to handle simultaneously the polarised beam and polarised target (cell–type), and (ii) establishing polarisation standards for double–polarised nuclear reactions at COSY energies. It is important to stress that, without these two steps, it will not be possible to realise the COSY–ANKE spin programme.

The proposal requires in TOTAL **four weeks** of beam time to determine the vector $C_{y,y}(C_{x,x})$ and tensor $C_{yy,y}$ spin correlation coefficients at two energies $T_d = 1.2\,\mathrm{GeV}$ and $T_d = 2.23\,\mathrm{GeV}$. In the framework of the PRESENT request, the collaboration asks for **two weeks** of beam time to carry out the first measurements at $T_d = 1.2\,\mathrm{GeV}$.

Contents

1 Introduction

In summer 2005 we submitted to the PAC a comprehensive document outlining our future plans for experiments involving polarised beams and targets to be performed with the ANKE facility [1], and this general programme was approved with high priority for the coming years at COSY.

We have shown that we can study successfully reactions with polarised beams of protons [2] and deuterons [3] and, in particular, proved that we can calibrate the vector and tensor polarisations of the deuteron beam [4]. Since the equipment needed is in position, it is now time to advance our programme by proposing experiments using a polarised target cell in conjunction with a polarised beam. This is the purpose of the present document.

In order to calibrate the polarisations of both the beam and target, it is necessary to measure in parallel reactions where the analysing powers are known. The ones chosen for this purpose are elastic deuteron–proton scattering and quasi–free $\vec{n}\vec{p} \to d\pi^0$, with a fast spectator proton. These reactions have high counting rates and characteristic kinematics, with two charged particles that can be detected. The experiment is crucial in: (i) teaching us how to handle simultaneously the polarised beam and polarised target (cell–type), and (ii) establishing polarisation standards for double–polarised nuclear reactions at COSY energies. It is important to stress that without these two steps it will not be possible to realise the COSY–ANKE spin programme [1].

We have already argued at length [5] that it is important to measure the Charge–Exchange (CE) breakup of polarised deuterons on a polarised hydrogen target. At low excitation energies E_{pp} of the final pp system, the observables in $\vec{d}\vec{p} \to \{pp\}n$ can be directly related to the spin–dependent neutron–proton charge–exchange amplitudes. Our measurement of the deuteron–proton spin correlation will thus allow us to determine the relative phases of these amplitudes and not just their overall magnitudes. This is the primary aim of our current proposal.

1.1 Motivation for the deuteron charge–exchange reaction

The complete investigation of the NN interaction requires precise data as input to a phase–shift analysis (PSA), from which the scattering amplitudes can be reconstructed. The PSA generally requires experiments with both beam and target particles polarised in the initial state, as well as the determination of the polarisation of one of the final state particles [6]. Experiments of this type have been carried out for the pp system up to about 3.0 GeV [7, 8]. Due to the absence of polarised neutron beams, much less work has been done on spin observables in elastic np scattering above 800 MeV [9, 10]. As a consequence, the PSA for isospin $I = 0$ are poorly tested in this region. Precise new data are needed in order to try to bridge the gap with the pp system. It has been shown that information can be obtained on the spin–dependent np elastic amplitudes near the backward direction (the charge–exchange region) by measuring the charge–exchange breakup of polarised deuterons on an unpolarised/polarised hydrogen target [11, 12] and it is this approach that we wish to pursue up to the maximum energy of the COSY deuteron beam, $T_d = 2.23$ GeV [5].

The experimental programme was divided into two parts:

1. Already in the first stage, we used unpolarised and polarised deuteron beams incident on an unpolarised hydrogen cluster target. The differential cross section gave only the overall intensity of the spin–dependent parts of the elementary CE process. The tensor polarised deuteron beam enabled us to separate the absolute values of three spin–dependent amplitudes.

2. Using transversely polarised deuterons incident on a polarised internal hydrogen gas target and measuring the spin–correlation coefficients opens the possibility of obtaining the relative phases between the amplitudes.

The present proposal covers the second part, where polarised and unpolarised deuteron beams will be utilised together with a polarised hydrogen target.

1.2 Achievements

The following milestones have been passed in the first stage of our programme:

1. Established the procedure for determining the vector and tensor polarisation components of the 1170 MeV deuteron beam by measuring the analysing powers of three different reactions: $\vec{d}p$ elastic scattering, $\vec{n}p \to d\pi^0$, and $\vec{d}p \to {}^3\mathrm{He}\,\pi^0$ [4].

2. At a beam energy of 585 MeV/A, our A_{xx} and A_{yy} measurements [3], led to the first determination of the amplitude ratios $|\varepsilon/\beta|$ and $|\delta/\beta|$ for the charge–exchange reaction for $q \leq 120\,\mathrm{MeV/c}$.

3. The commissioning results of the polarised internal target (PIT) are described in detail in section 4.4 but the main points are:

    - After its first installation in the summer of 2005, commissioning studies were carried out. These included storage cell tests to determine the dimensions of the COSY beam. The cell, which was made from pure aluminium foil, has a length of 400 mm, and a cross section of $20 \times 20\,\mathrm{mm}^2$.
    - In November 2005, tests with such a storage cell were undertaken using polarised hydrogen atoms from the polarised atomic beam source (ABS). The COSY beam consisted of electron–cooled unpolarised protons, stacked at injection, and accelerated to $T_p = 600\,\mathrm{MeV}$. It was possible to store 1.5×10^{10} protons in the flat top.
    - In March 2006, a first asymmetry measurement was carried out with a COSY beam of unpolarised 831 MeV protons and a polarised hydrogen target.
    - The analysis of the $pp \to pp\pi^\circ$ and $pp \to pn\pi^+$ reactions showed that events from the extended target can be cleanly identified in the ANKE forward detector system when there are two charged particles in the final state.
    - The target thickness with a hydrogen beam from the ABS injected into the cell in hyperfine (HF) state–**1** ($\mathrm{m_I} = \mathrm{m_J} = +\frac{1}{2}$) was estimated to be about 1.2×10^{13} H atoms/cm^2.
    - An average target polarisation of $P = 0.44\pm0.03$ was measured to be compared to the expected $P = 0.53 \pm 0.02$.

1.3 In progress

In order to complete the analysis of the polarised deuteron experiment it is necessary:

- to finish the acceptance calculation for CE deuteron breakup reaction with a three–body final state (2$\to$3) and determine the luminosity from three different reactions (dp elastic scattering, $np \to d\pi^0$, and $dp \to {}^3\mathrm{He}\,\pi^0$),
- to obtain the charge–exchange cross section and hence
- to derive the absolute values of ε, δ, and β rather than mere ratios.

2 Spin Formalism and Dynamics

2.1 Observables in double–polarisation measurements

2.1.1 Deuteron–proton collisions

Ohlsen has discussed in detail the observables that can be accessed when a polarised spin-1 particle collides with polarised spin-$\frac{1}{2}$ target [13]. In a right–handed coordinate system, with z pointing along the beam direction, y being perpendicular to the reaction plane, and x lying therein, the differential cross section σ for a dp–induced reaction can be written:

$$\begin{aligned}\sigma/\sigma_0 = 1 \quad &+ \quad Q_y A_y^p + \tfrac{3}{2} P_y A_y^d \\ &+ \quad \tfrac{2}{3} P_{xz} A_{xz}^d + \tfrac{1}{3}(P_{xx}A_{xx} + P_{yy}A_{yy} + P_{zz}A_{zz}) \\ &+ \quad \tfrac{3}{2}(P_xQ_xC_{x,x} + P_xQ_zC_{x,z} + P_yQ_yC_{y,y} + P_zQ_xC_{z,x} + P_zQ_zC_{z,z}) \\ &+ \quad \tfrac{1}{3}(P_{xx}Q_yC_{xx,y} + P_{yy}Q_yC_{yy,y} + P_{zz}Q_yC_{zz,y}) \\ &+ \quad \tfrac{2}{3}(P_{xy}Q_xC_{xy,x} + P_{xy}Q_zC_{xy,z} + P_{yz}Q_xC_{yz,x} + P_{yz}Q_zC_{yz,z}), \end{aligned} \tag{1}$$

where the polarised deuteron beam is described by the components P_i and P_{ik}, and the polarised hydrogen target by the components Q_i with $i, k = x, y, z$; σ_0 is the unpolarised cross section. The single polarisation observables are the proton analysing power A_y^p and the deuteron vector and tensor analysing powers A_y^d and A_{ik} $(i, k = x, y, z)$. In addition there are the vector and tensor spin–correlation coefficients $C_{i,k}$ and $C_{ik,j}$.

In our set–up, both the target proton and incident deuteron are polarised perpendicularly to the plane of the COSY ring, with polarisation Q and (P_z, P_{zz}) respectively. In general the reaction plane lies at an azimuthal angle ϕ with respect to the COSY plane, where ϕ is measured *clockwise* from the positive x-axis, looking along the beam direction. In this system the differential cross section becomes [13, 14]

$$\begin{aligned}\sigma/\sigma_0 \quad &= \quad 1 + Q\,A_y^p\cos\phi + \tfrac{3}{2}P_zA_y^d\cos\phi + \tfrac{1}{4}P_{zz}\left[(A_{yy}+A_{xx}) + (A_{yy}-A_{xx})\cos 2\phi\right] \\ &+ \ \tfrac{3}{4}P_zQ\left[(C_{y,y}+C_{x,x}) + (C_{y,y}-C_{x,x})\cos 2\phi\right] \\ &+ \tfrac{1}{4}P_{zz}Q\left[(\tfrac{1}{2}C_{xx,y} + \tfrac{1}{2}C_{yy,y} + C_{xy,x})\cos\phi + (\tfrac{1}{2}C_{xx,y} - \tfrac{1}{2}C_{yy,y} + C_{xy,x})\cos 3\phi\right]. \end{aligned} \tag{2}$$

2.1.2 Nucleon–nucleon collisions

Since our calibration of the beam and target polarisations will rely heavily on the measurements of quasi–free $np \to d\pi^0$ production, we shall also need the corresponding formula for the collision of two spin-$\frac{1}{2}$ particles. For beam and target polarisations P and Q normal to the COSY plane, the azimuthal angular dependence is [13]:

$$\sigma/\sigma_0 = 1 + \left(A_y^P P + A_y^Q Q\right)\cos\phi + \tfrac{1}{2}PQ\left[(A_{y,y}+A_{x,x}) + (A_{y,y}-A_{x,x})\cos 2\phi\right]. \tag{3}$$

Here $A_{x,x}$ and $A_{y,y}$ are spin–correlation parameters and A_y^P and A_y^Q are analysing powers for polarised beam and target, respectively. Note that for cases such as pp elastic scattering or $pn \to d\pi^0$, where there is a unique isospin, one has $A_y^P = A_y^Q$.

2.2 Impulse approximation dynamics for deuteron charge exchange

We present here a simplified description of the $\vec{d}\vec{p} \to \{pp\}n$ charge exchange reaction in impulse approximation, assuming that the final pp state is purely ${}^1S_0$ [12]. This identification is largely valid for low excitation energy $E_{pp} < 3$ MeV of the outgoing diproton and low three-momentum transfers q from proton to neutron. In our full analysis we estimate reliably the dilution of the analysing power signals due to the presence of P and higher waves in the final pp system [3, 15].

The amplitude of the elementary $np \to pn$ reaction in the cm system can be written in terms of five scalar amplitudes

$$f_{np} = \alpha + i\gamma(\boldsymbol{\sigma}_n + \boldsymbol{\sigma}_p)\mathbf{n} + \beta(\boldsymbol{\sigma}_n \cdot \mathbf{n})(\boldsymbol{\sigma}_p \cdot \mathbf{n}) + \delta(\boldsymbol{\sigma}_n \cdot \mathbf{m})(\boldsymbol{\sigma}_p \cdot \mathbf{m}) + \varepsilon(\boldsymbol{\sigma}_n \cdot \mathbf{l})(\boldsymbol{\sigma}_p \cdot \mathbf{l}), \quad (4)$$

where $\boldsymbol{\sigma}_n$ and $\boldsymbol{\sigma}_p$ are the Pauli matrices for neutron and proton, respectively. The orthogonal unit vectors are defined in terms of the initial ($\mathbf{k}$) and final ($\mathbf{k}'$) momenta as

$$\mathbf{n} = \frac{\mathbf{k} \times \mathbf{k}'}{|\mathbf{k} \times \mathbf{k}'|}, \quad \mathbf{m} = \frac{\mathbf{k}' - \mathbf{k}}{|\mathbf{k}' - \mathbf{k}|}, \quad \mathbf{l} = \frac{\mathbf{k}' + \mathbf{k}}{|\mathbf{k}' + \mathbf{k}|}\,.$$

The amplitudes are normalised such that the elementary $np \to pn$ differential cross section has the form

$$\left(\frac{d\sigma}{dt}\right)_{np\to pn} = I_{np} = |\alpha|^2 + |\beta|^2 + 2|\gamma|^2 + |\delta|^2 + |\varepsilon|^2\,, \quad (5)$$

where α is the spin–independent amplitude, γ is a spin–orbit term, and β, δ, and ε are the spin–spin amplitudes. The one–pion–exchange pole is contained purely in the δ amplitude and this gives rise to its very rapid variation with momentum transfer, which influences very strongly our results.

In impulse approximation, *i.e.* single $np \to pn$ scattering, the resulting deuteron charge–exchange amplitude depends only upon the spin–dependent parts of f_{np}, *i.e.* β, γ, δ and ε [12]. The form factor describing the transition from a deuteron with spin–projection λ to a ${}^1S_0$–state of the final pp pair contains two terms

$$\begin{aligned} S^+(k, \tfrac{1}{2}q) &= F_S(k, \tfrac{1}{2}q) + \sqrt{2}F_D(k, \tfrac{1}{2}q)\,, \\ S^-(k, \tfrac{1}{2}q) &= F_S(k, \tfrac{1}{2}q) - F_D(k, \tfrac{1}{2}q)/\sqrt{2}\,. \end{aligned} \quad (6)$$

The S^+ and S^- denote the longitudinal ($\lambda = 0$) and transverse ($\lambda = \pm 1$) form factors. The matrix elements F_S and F_D can be expressed in terms of the S– and D–state components of the deuteron wave function $u(r)$ and $w(r)$ and the $pp({}^1S_0)$–scattering wave function $\psi_k^{(-)}(r)$ as

$$F_S(k, \tfrac{1}{2}q) = \langle \psi_k^{(-)} | j_0(\tfrac{1}{2}qr) | u \rangle\,, \quad (7)$$

$$F_D(k, \tfrac{1}{2}q) = \langle \psi_k^{(-)} | j_2(\tfrac{1}{2}qr) | w \rangle. \quad (8)$$

Here k is the pp relative momentum, corresponding to an excitation energy $E_{pp} = k^2/m$, where m is the proton mass. Let us denote the ratio of the transition form factors by

$$R = S^+(k, \tfrac{1}{2}q)\Big/ S^-(k, \tfrac{1}{2}q) \quad (9)$$

and the sum of the renormalised modulus–squares of the amplitudes by

$$I = |\beta|^2 + |\gamma|^2 + |\varepsilon|^2 + |\delta|^2 R^2. \quad (10)$$

Impulse approximation applied to $dp \to (pp)_{{}^1S_0}n$ then leads to the following predictions for the differential cross section, deuteron analysing powers, and spin–spin correlation parameters $C_{y,y}$, $C_{x,x}$ [15, 16]:

$$\begin{aligned}
\frac{d^4\sigma}{dtd^3k} &= \tfrac{1}{3}I\left\{S^-(k,\tfrac{1}{2}q)\right\}^2 ,\\
I\,A_y^d &= 0\,,\\
I\,A_y^p &= -2\Im(\beta^*\gamma)\,,\\
I\,A_{xx} &= |\beta|^2+|\gamma|^2+|\varepsilon|^2-2|\delta|^2R^2\,,\\
I\,A_{yy} &= |\delta|^2R^2+|\varepsilon|^2-2|\beta|^2-2|\gamma|^2\,,\\
I\,C_{y,y} &= -2\Re(\varepsilon^*\delta)R,\\
I\,C_{x,x} &= -2\Re(\varepsilon^*\beta).
\end{aligned} \tag{11}$$

Within this approximation, a measurement of the differential cross section, A_{xx}, and A_{yy} allows the extraction of $|\beta|^2+|\gamma|^2$, $|\delta|^2$, and $|\varepsilon|^2$ over a range of values of q near the forward direction. As seen from Fig. 1, and reported in Ref. [3], we have shown that this can be successfully done at 1170 MeV for $q \leq 130$ MeV/c, though there is still some work to be done on the acceptance corrections to obtain the absolute cross sections from our data. The values of A_y^d are consistent with zero for all momentum transfers and that provides further support for the impulse–approximation interpretation.

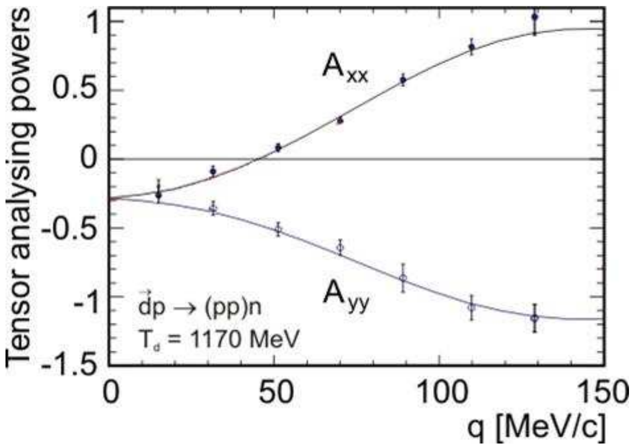

Figure 1: Cartesian tensor analysing powers A_{yy} (open symbols) and A_{xx} (closed) of the $\vec{d}p \to (pp)n$ reaction for $E_{pp} < 3$ MeV at T_d=1170 MeV compared to the impulse approximation predictions. Details can be found in Ref. [3].

On the other hand, Eq. (11) shows that in order to get information on the relative phases of the np charge–exchange amplitudes, one needs to measure the spin–spin correlation parameters using polarised protons as well as deuterons. This is the major purpose of the proposed experiment.

2.2.1 Spin–correlation predictions

Numerical predictions have been made for the transverse spin–correlation coefficients for the deuteron charge–exchange reaction in impulse approximation and the results are shown in Fig 2.

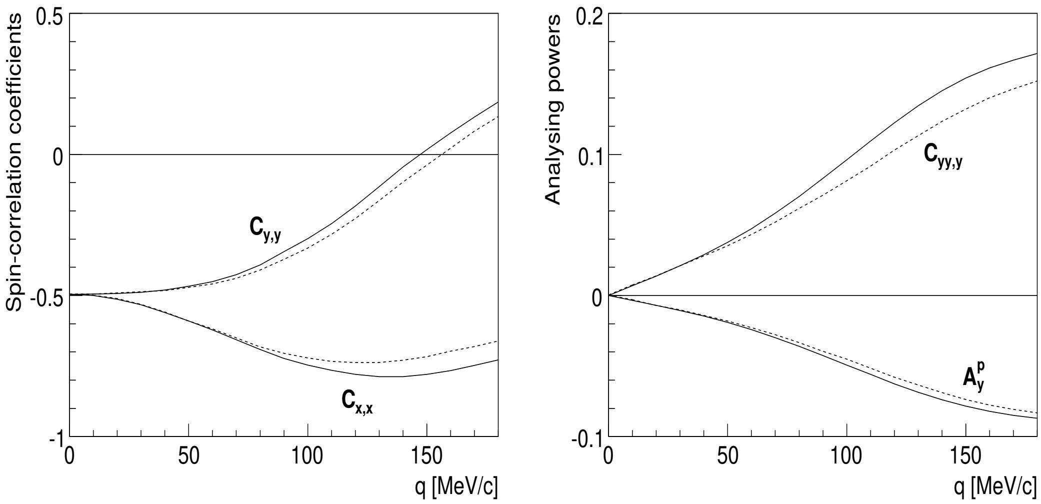

Figure 2: The spin–correlation coefficients (left panel) and analysing powers (right panel) in the CE reaction at 585 MeV/nucleon for cuts in excitation energy of $E_{pp} < 1$ MeV (solid line) and $E_{pp} < 3$ MeV (dashed line).

The predicted $C_{x,x}$ and $C_{y,y}$ are both expected to be very large and show considerable structure over the ANKE measurement range. At $q = 0$, $C_{y,y} = C_{x,x} \approx -0.5$ but at $q = 140\,\text{MeV/c}$ $C_{y,y}$ passes through zero and $C_{x,x} = -0.85$. This comes about because of the spin–spin amplitudes β, δ, and ε all having rather similar phases. In the forward direction $\beta = \delta$ and ε is a bit smaller. On the other hand $\delta \approx 0$ for $q = m_\pi$. Therefore, using Eq. (11), all the behaviour seen in the Fig. 2 can be easily understood. It should be stressed that we are quite fortunate to have found such a large (predicted) signal with such an interesting behaviour.

In impulse approximation $A_y^d = 0$ for a final ${}^1S_0$–state but the proton analysing power need not vanish. In the ${}^1S_0$ limit the tensor spin–correlation is linked to the analysing power through: $C_{yy,y} = -2A_y^p$. In the right hand side picture it is seen that this relation is well respected in the $E_{pp} < 1$ MeV range. However, as the excitation energy increases, there is a bit more dilution of the $C_{yy,y}$ signal than the A_y^p through the production of P and higher waves that are included in the calculations. Unfortunately, the A_y^p prediction is very small and it will be hard to get a very precise measurement of it. The lack of some smoothness in the graphs above 150 MeV/c is at least in part physical, arising from the rapid variation and change of sign of the δ amplitude around here.

3 Beam and Target Polarimetry

3.1 Polarimetry with the quasi–free $\vec{n}p \to d\pi^0$ reaction: (P_z)

Due to isospin invariance, the neutron analysing power in the $\vec{n}p \to d\pi^0$ reaction should be identical to that of the proton in $\vec{p}p \to d\pi^+$, for which extensive data compilations are available [17]. As shown by our earlier results [4], which are presented in Fig. 3, the agreement of our result with the shape of the SAID predictions is very good for both small and large deuteron cm angles. This led to a determination of the vector polarisation of the deuteron beam since, for the small Fermi momenta investigated here, there is a one–to–one relation between the deuteron and constituent neutron polarisation. The value of P_z so deduced was completely consistent with that obtained from elastic $\vec{d}p$ scattering. This result was also in line with the EDDA measurements of the vector polarisation of the deuteron beam at lower energies [4]. Within small error bars, typically 2%, there was no sign of any effect arising from the tensor polarisation of the deuteron beam. This is as expected for a quasi–free reaction and provides an extra check on the systematics.

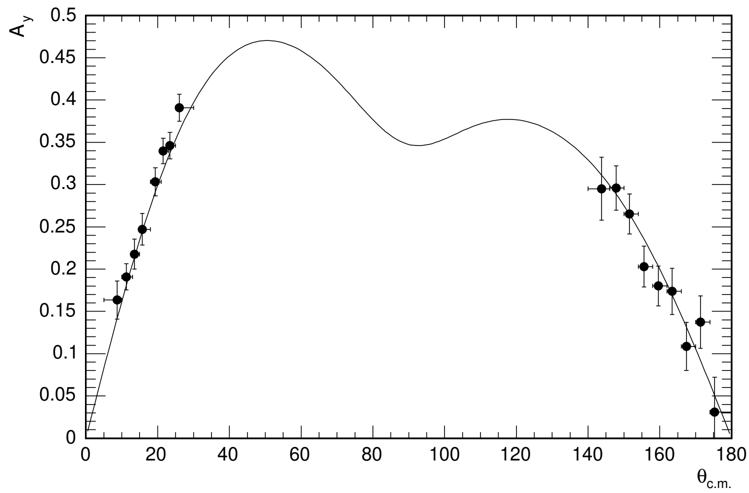

Figure 3: Analysing power of the $\vec{n}p \to d\pi^0$ at $\frac{1}{2}T_d$ =585 MeV [4] compared to the SAID predictions [17] for $\vec{p}p \to d\pi^+$ at this energy.

For the new experiment, using the unpolarised spin–mode of the deuteron beam, *i.e.* $P = 0$ in Eq. (3), the ϕ–dependence of the differential cross section allows one to extract the unpolarised σ_0 and also the combination QA_y^Q. The known values of the analysing power of the $\vec{p}p \to d\pi^+$ [17] would then lead to the determination of the polarisation Q of the hydrogen target.

For spin modes where the vector polarisation of the deuteron beam is non–zero, the $\cos\phi$ term in Eq. (3) is sensitive to the combination $(P+Q)$, which provides two measurements of P, by using the information from target spin–up and spin–down. In practice, the values of P and Q will be obtained from a simultaneous combined fit of information from all the beam and target spin modes; measurements with an unpolarised target are not necessary. It is interesting to note that the relative calibration of the beam and target polarisations does not depend upon the value of analysing power assumed. As by–products of this measurements we will be able to extract the spin–correlation coefficients $A_{x,x}$ and $A_{y,y}$ for $\vec{n}\vec{p} \to d\pi^0$ at both large and small production angles. These quantities, which are symmetric in $\cos\theta$, are both expected to be very large (≈ -0.9) in our angular domain over a wide range of incident energies [17]. Nevertheless, we will provide data at smaller angles than those that exist in the literature [18].

3.2 Polarimetry with elastic deuteron–proton scattering: (P_z, P_{zz})

Unlike the case of $np \to d\pi^0$, the acceptance of the ANKE system for small angle $dp \to dp$ is limited to regions that are very close to $\cos\phi = \pm 1$. With an unpolarised deuteron beam, Eq. (2) shows that in this case one can determine the unpolarised cross section as well as the combination $A_y^p Q$. However, the measurements of the proton analysing power in this reaction show that A_y^p is not large and not obtained with adequate precision in our energy and angular domain to provide the necessary calibration standard [19]. Inverting the procedure and taking the value of Q from the quasi–free $n\vec{p} \to d\pi^0$ analysis, results with the unpolarised beam will give us a measurement of A_y^p.

By weighting the data for target spin–up and spin–down with the appropriate values of Q, it is possible to extract the results that would correspond to an unpolarised target. In this case, Eq. (2) simplifies to

$$\sigma/\sigma_0 = 1 + \tfrac{3}{2} P_z A_y^d \cos\phi + \tfrac{1}{4} P_{zz}\left[(A_{yy} + A_{xx}) + (A_{yy} - A_{xx})\cos 2\phi\right] \tag{12}$$

We then rely, as in our previous work, on the measurements of the deuteron vector and tensor analysing powers carried out at SATURNE [20] and Argonne [21] in order to provide a measurement of P_{zz} and a further determination of P_z.

In a final step, taking $\phi = 0^\circ$ and 180° in Eq. (2), the data with polarised beam and target will fix the values of the spin–spin correlation parameters $C_{y,y}$ and $(C_{xx,y} + 2C_{xy,x})$.

4 Experimental Facilities

4.1 The ANKE detection system

We consider here the possibility of studying the charge–exchange deuteron–breakup reaction using the ANKE spectrometer. This apparatus is described in Ref. [22] and we shall merely discuss here the details of its additional features.

The reactions that are relevant to this polarisation study are:

- $dp \to (pp)n$ producing a fast pair of protons with low excitation energy,
- Quasi–free $np \to d\pi^0$ with a fast spectator proton, and
- $dp \to dp$ at small deuteron angles.

The first two reactions can be measured using principally the information obtained from the ANKE Forward Detector (FD) system [3, 4]. This comprises a set of three multi-wire proportional chambers (MWPCs) and a three–plane scintillation hodoscope, consisting of vertically oriented counters (8 in the first plane, 9 in the second, and 6 in the third). The hodoscope system is capable of detecting pairs of particles, such as the protons emerging from the deuteron charge–exchange reaction $dp \to (pp)n$ [3].

Though deuteron–proton elastic scattering can also be identified on the basis solely of the FD information, the coincidence measurements with the slow recoil proton being detected in a Silicon Tracking Telescope (STT) yields more precise information [4]. We should note here that this is true for the measurements with cluster target, but that it has not yet been proven with a long cell target.

4.2 Silicon Tracking Telescope

4.2.1 Design parameters

For the identification and tracking of slow protons and deuterons emerging from the target, a Silicon Tracking Telescope (STT) has been developed that can be operated inside the ultra–high vacuum of the accelerator [23]. The basic concept of the STT combines particle identification with tracking over a wide range in energy. The tracking is accomplished by three layers of double–sided micro–structured silicon strip detectors that can be placed close to the target inside the vacuum chamber. The set–up of the STT is shown in Fig. 4.

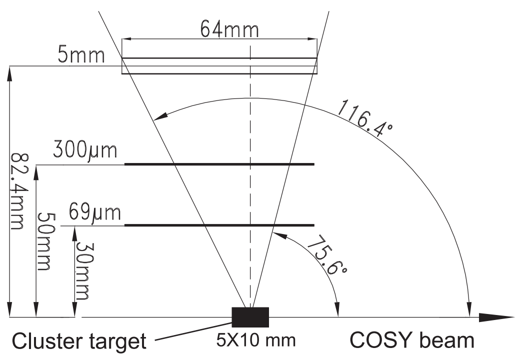

Figure 4: Top view of the Silicon Tracking Telescope (STT), consisting of three layers of different thickness. The approximate extension of the cluster target beam in the x–z plane is indicated, along with the approximate polar angles covered.

Measuring the energy loss in the individual layers allows the identification of stopped particles by the $\Delta E/E$ method. A particle is registered when it passes through the inner layer and is stopped in the second, so that the minimum energy of a particle that can be tracked is determined by the thickness of the innermost layer. The maximum energy of tracked particles is given by the range within the telescope and hence by the total thickness of all detection layers. The primary design goal in the development of the STT was therefore to combine the thinnest possible innermost with the thickest available outermost layer of silicon detector.

The new STT employs the well–established thickness of the first generation system [24], but overcomes the limited tracking capabilities by using double–sided micro–structured detectors. The angular coverage in the forward hemisphere was small in our previous experiment [4], because the position of the STT with respect to the target was optimised to detect slow recoil protons in the backward hemisphere. Nevertheless, protons emitted at angles from about 75° to 80° were unambiguously identified in the STT in coincidence with elastically scattered deuterons in the FD.

The new STT facilitates $\Delta E/E$ proton identification from 2.5 up to 40 MeV with an energy resolution of 150–250 keV (FWHM). Particle tracking is possible over a wide range of energies with an angular resolution varying from 1° to 6° (FWHM). The resolution is limited by angular straggling within the detectors and therefore depends on particle type, energy, and track inclination. The geometrical limit is defined by the strip pitch (ranging from 400 to 666 μm) and the distances between the detectors.

The STT has self–triggering capabilities. It identifies a particle's passage within 100 ns and provides the possibility for fast timing coincidences with other detector components of the ANKE spectrometer, whereby accidental coincidences can be suppressed significantly. The high rate capabilities of the STT will be especially important for some of the polarisation experiments [1], because two or more STTs have then to be placed in the forward hemisphere. The recent development of very thick (> 10 mm) double–sided micro–structured Si(Li) detectors will allow us to extend further the accessible energy range of the STT.

4.2.2 Status: Application with the long cell-type target

In order to reconstruct the momentum of a particle from the track information in the ANKE detection systems, the vertex of the reaction must be determined. This is a non–trivial task for an extended storage cell target that will be up to 40 cm in length. By having additional track(s) in the Silicon Tracking Telescopes close to the ANKE target region inside the COSY vacuum, the vertex can be reconstructed precisely.

Depending upon the requirements of individual experiment, four to six telescopes can be equipped with different sets of silicon detectors and be positioned around the target region to serve several purposes:

- Spectator proton detector: Low energy protons from a deuterium target will be identified and tracked in the range $2.5 < T_p < 35$ MeV. Each telescope covers about 10% of the geometrical acceptance.

- Vertex detector: One track in a Silicon Tracking Telescope defines the vertex in two coordinates (along and perpendicular to the beam) with a precision of about 1 mm. The third coordinate can only be fixed by using the spatial resolution of the ANKE detection system, which gives about 10 mm. Only for reactions such as $pd \to n\{pp\}$, where there are two tracks inside the telescopes, can one obtain a full 3–D vertex reconstruction with a precision of about 1 mm. In such a case, any reaction occurring on the walls of the storage cell can be easily identified.

- Polarimeter: Two protons in the telescopes from the *pp* elastic or quasi–elastic scattering allow one to analyse the polarisation along the storage cell in parallel with the main experiment.

These delicate instruments need be properly tested in the new polarised internal target (PIT) environment, and for this purpose the PAC #31 recommended one week of machine development plus one week of beam time, which is scheduled in Jan/Feb 2007 (see proposals #159 [25] and #146 [26]).

4.3 Actual configuration of the COSY polarised deuterium ion source

Mode	P_z	P_{zz}	I_0	RFT_1	RFT_2	RFT_3	States	N_+	N_0	N_-
0	0	0	1	Off	Off	Off	1,2,3	$\frac{1}{3}$	$\frac{1}{3}$	$\frac{1}{3}$
1	$-\frac{2}{3}$	0	1	Off	Off	On	2,3,4	0	$\frac{1}{3}$	$\frac{2}{3}$
2	$\frac{1}{3}$	1	1	Off	$2 \rightleftharpoons 6$	Off	1,3,6	$\frac{2}{3}$	0	$\frac{1}{3}$
3	$-\frac{1}{3}$	-1	1	Off	$2 \rightleftharpoons 6$	On	2,4,5	0	$\frac{2}{3}$	$\frac{1}{3}$
4	$\frac{1}{3}$	-1	1	Off	$3 \rightleftharpoons 5$	Off	1,2,5	$\frac{1}{3}$	$\frac{2}{3}$	0
5	$-\frac{1}{3}$	1	1	Off	$3 \rightleftharpoons 5$	On	3,4,6	$\frac{1}{3}$	0	$\frac{2}{3}$
6	0	1	$\frac{2}{3}$	26	Off	Off	1,3	$\frac{1}{2}$	0	$\frac{1}{2}$
7	$\frac{1}{2}$	$-\frac{1}{2}$	$\frac{2}{3}$	26	$3 \rightleftharpoons 5$	Off	1,5	$\frac{1}{2}$	$\frac{1}{2}$	0
8	$\frac{1}{2}$	$-\frac{1}{2}$	$\frac{2}{3}$	35	Off	Off	1,2	$\frac{1}{2}$	$\frac{1}{2}$	0
9	-1	1	$\frac{2}{3}$	35	Off	On	3,4	0	0	1
10	1	1	$\frac{2}{3}$	35	$2 \rightleftharpoons 6$	Off	1,6	1	0	0
11	0	-2	$\frac{2}{3}$	35	$2 \rightleftharpoons 6$	On	2,5	0	1	0
12	$-\frac{1}{2}$	$-\frac{1}{2}$	$\frac{2}{3}$	26	Off	On	2,4	0	$\frac{1}{2}$	$\frac{1}{2}$
13	$\frac{1}{2}$	$-\frac{1}{2}$	$\frac{2}{3}$	26	$3 \rightleftharpoons 5$	On	2,6	$\frac{1}{2}$	$\frac{1}{2}$	0

Table 1: Deuteron polarisation states available from the polarised deuterium ion source.

Table 1 shows the fourteen different polarisation states that can presently be provided by the COSY polarised source for deuterium D^- ions. All states are available without breaking the source vacuum and can be delivered in any desired sequence. The final combination of states depends on the proper combination of static and rf fields for the transition units.

The frequency of the transition units 1 and 2 can be changed in the range of 325 to 400 MHz in a few minutes to allow additional transitions (which are not given in Table 1). A transition unit tuned to 328 MHz can provide the single state 1 (as RFT1), or pure vector polarisation +2/3 (as RFT2). The tuning parameters of the five possible transitions are the main magnetic field, the rf amplitude, and two correction coils for the magnetic gradient. The Wien Filter provides two additional parameters, magnetic field and rotation angle for the spin alignment.

The routine preparation of a COSY run includes the requirement that all transition units are separately tested for maximum intensity modulation by being installed between the hexapoles of the atomic beam part. Usually an intensity modulation in excess of 90% of the limiting value of 1/3, or 2/3 respectively, has been reached for all transitions, which is close to the expected value.

In the near future the installation of a Lamb–Shift Polarimeter (LSP), a copy of that used at the ANKE PIT, will be started. In a set–up with a decelerating structure, a gas target in a strong magnetic field, a deflector and a Cs neutraliser, the nuclear polarisation of the polarised H^- and D^- beams can be analysed. Each parameter is again scanned with a statistical precision of 2% for the polarisation at the beginning of an experimental run. Within two hours each transition unit can be tuned to about 70% of its nominal performance for vector polarisation using the polarimeter in the injection beam line.

Using the EDDA detector with a proper calibration, vector and tensor polarisation data with high statistical precision are accessible. That was achieved for the *SPIN@COSY* experiment during the last run in May 2006 and allowed one to improve the vector polarisation from 70% to 86% by scanning the polarisation against the main field of the transition units. The results for pure tensor polarisation are still only 30–50% of expectation.

The current proposal will use the polarised deuteron beam from the COSY ion source. The scheme will consist of five different polarisation states, one unpolarised state and four combinations of vector and tensor polarisation, as shown in Table 2.

	theoretical maximum		
	vector	tensor	Intensity
Mode	P_z	P_{zz}	I_0
0	0	0	1
6	0	+1	2/3
9	−1	+1	2/3
10	+1	+1	2/3
11	0	−2	2/3

Table 2: Modes of the polarised deuterium ion source. The intensity modulations between the different modes constitute a compromise in order to achieve higher polarisations. I_0 refers to the maximum number of deuterons delivered by the source and stored in COSY. At the deuteron energies of our experiment, we expect $I_0 = 10^{10}$ deuterons.

For each injection into COSY, the polarised ion source can be switched to a different polarisation state. The duration of a cycle is sufficiently long to ensure stable conditions for the injection of the next state. After the fifth state, the source will be reset to the first mode and the pattern repeated. The ANKE data acquisition system receives status bits from the source, latched during injection, to ensure the correct identification of the polarisation states during the experiment. In a similar way the polarisation information is stored for the ABS beam.

The vector (P_z) and tensor (P_{zz}) polarisations of a deuteron beam have been measured using elastic deuteron–carbon scattering at 75.6 MeV and deuteron–proton scattering at 270 MeV [4]. After acceleration to 1170 MeV inside the COSY storage ring, the polarisations of the deuterons were re-measured by studying the analysing powers of a variety of nuclear reactions. The overall precisions obtained were about 4% for both P_z and P_{zz}. Though all the measurements were consistent with the absence of depolarisation during acceleration, only an upper limit of about 6% could be placed on such an effect due to the uncertainties in the calibrations at lower energies.

The present experiment will be the first to provide measurements of the vector and tensor polarisation of the stored deuteron beam interacting with the polarised hydrogen target in COSY.

4.4 Polarised Internal Target and Lamb–Shift Polarimeter: Status

The polarised internal target (PIT) system at ANKE consists of an atomic beam source (ABS) feeding a storage cell and a Lamb–shift polarimeter (LSP). The status of the different components is discussed here.

For the PIT commissioning and for the first experiments, four weeks of beam time towards the end of 2005 and beginning 2006 were granted by PAC No. #29 and #30 (COSY experiment No. 146) and this time has been used for the activities described in the beam request [26]. During the last period, the results achieved demonstrated that the ABS target is approaching its operational status and some high cross section reactions may already be investigated using it. One week of machine development plus one week of beam time were approved for the proposal [26]. In the first week, in close collaboration with the accelerator staff, installation of and beam development with the ABS cell–target should be performed. The second week should be dedicated to a pilot measurement of polarised deuteron breakup on a polarised hydrogen target (see minutes of PAC #31).

4.4.1 Polarisation of the $\vec{\mathrm{H}}$ jet target

The polarisation of the $\vec{\mathrm{H}}$ beam from the ABS was measured in the laboratory and values of $P_+ = +0.898 \pm 0.004$ and $P_- = -0.900 \pm 0.005$ were obtained [27]. It had been planned to populate either the pure $\mathrm{m_I} = \mathrm{m_J} = +\frac{1}{2}$ hyperfine (HF) state–**1** for positive polarisation (or the pure $\mathrm{m_I} = \mathrm{m_J} = -\frac{1}{2}$ state–**3** for negative polarisation) by using both medium and weak field rf transition units. A failure of the weak field rf transition unit, probably caused by insufficient magnetic shielding, forced us to populate the mixed HF state–**2** with $\mathrm{m_I} = -\frac{1}{2}$ and $\mathrm{m_J} = +\frac{1}{2}$ to produce negative polarisation by switching the sign of the magnetic field gradient in the medium–field rf transition unit. The magnetic field in the jet axis at the height of the COSY beam has been measured as 165 G for a current of 563 A applied during the experiment to produce the field in the D2 gap. The full positive polarisation is maintained with the population of the pure HF state. For the negative polarisation, however, one expects a reduction by a factor 0.32 in the field of 165 G, which lies appreciably lower than the critical field of 507 G for hydrogen (see e.g. [28]). Thus, the measured value of -0.9 for the negative polarisation in the jet target is expected to be reduced to about -0.31.

The $p\vec{p} \to d\pi^+$ reaction has been used to measure the polarisation of the $\vec{\mathrm{H}}$ jet (see status report [29]). To minimise systematic errors, the polarisation of the jet within the runs was changed every 5 s by switching the sign of the gradient field in the medium–field rf transition unit. The result is shown in Fig. 5. Assuming that both polarisation P_+ and P_- were equal, an average target polarisation of $P = 0.44 \pm 0.03$ was measured, to be compared to an expectation lying in the $P = 0.51 - 0.55$ range.

4.4.2 ABS measurements with the LSP

The use of the Lamb-shift polarimeter at the ANKE target position for the tuning of the rf–transition units and measuring the polarisation of the target gas by effusing of a sample of the gas from the storage cell had to be postponed. Preliminary results of nuclear polarisation measurements in the laboratory demonstrated the feasibility of the method. The sensitivity, however, has to be substantially enhanced to achieve the envisaged accuracy. Therefore, in the forthcoming beam time (Jan/Feb 2007) the LSP will be used in a modified geometry. This already allowed polarisation measurements of the direct ABS beam and thus enabled on–line tuning of the rf–transition units in the laboratory [30]. For this purpose the ABS beam, after crossing the COSY beam, will go through a strong

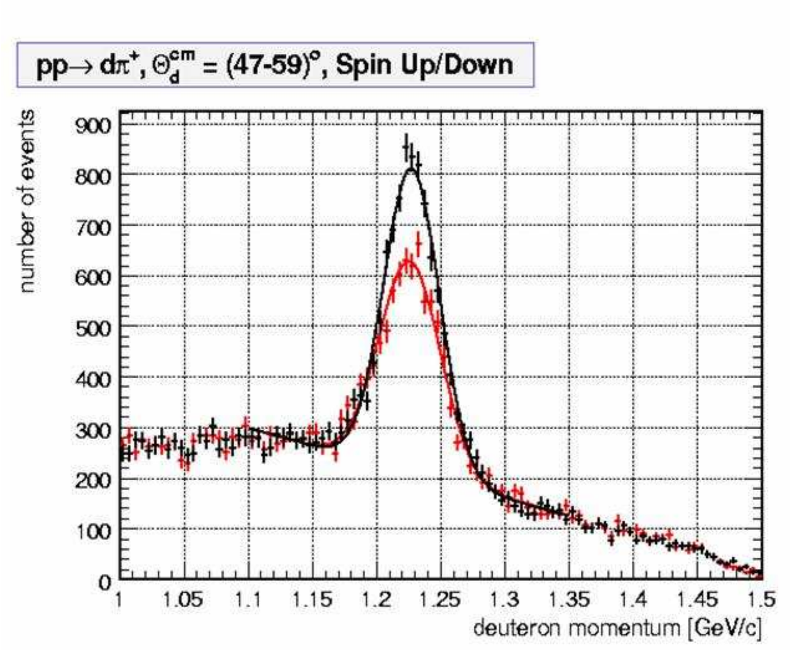

Figure 5: Identification of the $p\vec{p} \to d\pi^+$ reaction from the jet polarisation measurements [29]

magnetic field ioniser that is mounted below the ANKE target chamber. The produced protons (deuterons) are deflected along a horizontal beam line. The residual atoms are pumped by a cryocatcher pump on top of the ioniser, a NEG (Non–Evaporable Getter) pump around the ionising volume, or a turbo pump at the deflector chamber. After the rotation of the quantisation axis by a Wien filter, the polarisation is measured with a combination of a Cs cell, a spin filter and quenching region [27]. The complete setup will be tested in October and implemented at COSY in December 2006.

5 Measurements at ANKE

As a first step, measurements with unpolarised deuterons incident on the unpolarised cluster target have been performed. The two fast protons, emitted into a narrow forward cone with momenta around half that of the deuteron beam, were detected in the ANKE forward detector system. During the same data–taking period, and in parallel to the unpolarised measurements, the polarised deuteron beam allowed us to carry out the first analysing powers studies, where we obtained a measurement of A_{xx} and A_{yy}, as given by Eqs. (2). For this purpose we took data by cycling through the polarisation modes 0, 1, 2, 3, 9, 10, 12, and 13, from the list in Table 1.

5.1 Monte Carlo simulations with a long target

5.1.1 FD acceptance for forward–going proton pairs

The MC simulations were carried out in order to estimate the efficiency of the ANKE forward detection system for registering two fast protons at small production angles when using the long ($20 \times 20 \times 380$ mm^3) cell–type target and proper density distribution along the cell.

The predicted horizontal acceptances of the set–up with an extended target for $T_d = 1.2\,\mathrm{GeV}$ and $1.6\,\mathrm{GeV}$ are shown in the two panels of Fig. 6 as functions of the laboratory production angle and magnetic rigidity. The vertical acceptance corresponds to $\pm 3.5°$. From the loci of the kinematics of the four reactions that we investigated in the previous polarisation study with a cluster target [3, 4] it was seen that all had reasonable acceptances over some angular domain. Comparison of the predictions for short and long targets shows that the general features of the acceptance are very similar, though the angular scale is a little wider for the cell target. Making use of the transverse positioning capability of the D2 magnet, the angle interval accepted in the forward detector can be optimised.

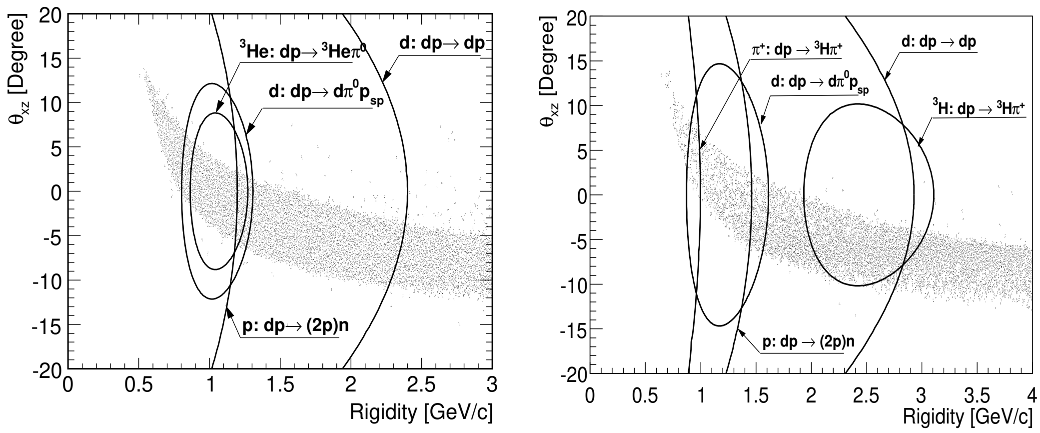

Figure 6: Predicted ANKE experimental acceptance for various nuclear reactions with an extended target at a deuteron beam energy of 1.2 GeV (left panel) and 1.6 GeV (right panel).

5.1.2 Reaction identification under PIT conditions

In this section the event identification for the dp–induced reactions when using a long cell target are demonstrated. This is done on the bases of both MC simulation and experimental information obtained in pp interaction, especially from the shape of the background from the cell walls, which is imitated through the use of N_2 gas in the cell.

Fig. 7 shows events where two charged particles were detected in the double–layer forward scintillation hodoscope during the previous commissioning beam–time. Unpolarised H_2 (N_2) gas was used in the ($20 \times 20 \times 380\ \mathrm{mm}^3$) cell with an incident beam of 831 MeV protons [29]. The figure shows the arrival–time differences for the two particles in the hodoscope (calculated after momentum and trajectory reconstruction under the assumption that both particles were protons) *versus* the measured difference of the two time signals from the scintillators. Thus, the two protons from the $pp \to pp\pi^0$ reaction lie along the diagonal, with other pairs being found elsewhere. A two–body reaction such as $pp \to d\pi^+$ yields isolated islands, with that of a fast π^+ and a slow deuteron being found to the right of the pp diagonal. The $p\pi^+$ events are smeared out due to the momentum carried by the undetected neutron from the $pp \to pn\pi^+$ reaction. Such off–diagonal events are, of course, mirrored above the diagonal.

Reactions in the N_2 gas in the cell are expected to show the same smearing of the ejectile momenta as reactions in the aluminium cell–wall material due the Fermi motion

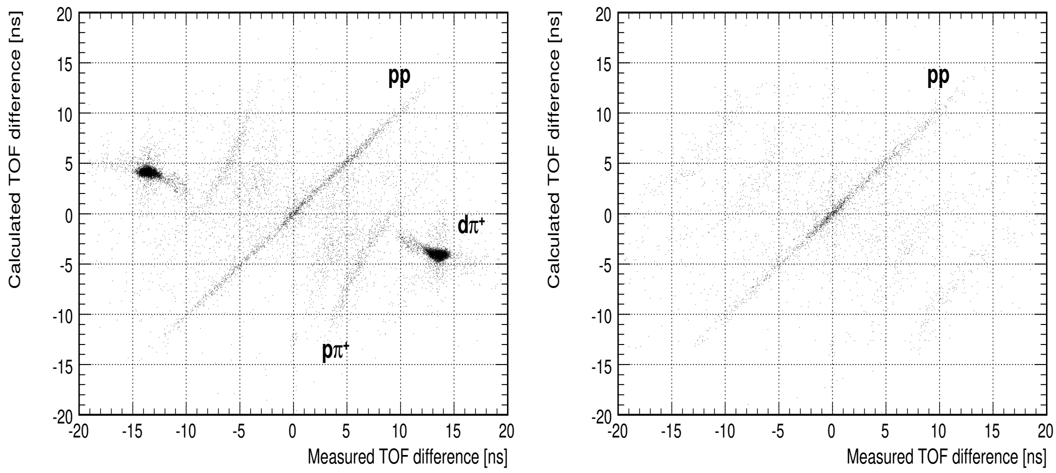

Figure 7: Time difference of the two detected charged particles, calculated under the assumption that both particles are protons, *versus* the measured time difference for events from 831 MeV protons and H_2 gas (left panel) and N_2 gas (right panel) in the storage cell of $20 \times 20\,\mathrm{mm}^2$ cross section and 380 mm length. These results were obtained during the commissioning beam–time.

of the nucleons [31]. The comparison of the results presented in the two panels of Fig. 7 shows strong effects for both $d\pi^+$ and $p\pi^+$ events. This should allow one to discriminate between reactions in the $\vec{\mathrm{H}}$ (and later also $\vec{\mathrm{D}}$) gas in the storage cell from wall events due to the different width in the momentum distribution. On the other hand, the narrow band of the pp events is very similar for H_2 and N_2 targets (and hence for the cell wall as well).

5.1.3 Missing–mass distributions for $pp \to pn\pi^+$ and $pp \to pp\pi^0$ reactions

Time-of-flight cuts applied to the distributions of Fig. 7 allow us to select $p\pi^+$ and pp candidates and hence to derive the missing–mass distributions of the $pp \to pn\pi^+$ and $pp \to pp\pi^0$ reactions that are presented in Fig. 8. Data with the hydrogen target (H_2) show prominent peaks corresponding to the production of a neutron or π^0, respectively. The background in both cases is very similar to that measured with the nitrogen target (N_2) and the natural assumption is that for hydrogen this comes from the cell walls.

It should be noted that the experimental data shown on Fig. 7 and Fig. 8 have been taken with the stochastically cooled proton beam [29]. During this test run, data were also taken in parallel with a non–cooled beam under the same experimental conditions. The results of the analysis show very similar missing–mass pictures for H_2 and N_2 targets. The shapes of the cooled and non–cooled data are very similar and the only major difference is that the signal/background ratio is made worse by about 10% by the absence of cooling.

5.1.4 Missing–mass distributions for $dp \to (pp)n$

The previous measurements with a proton beam and hydrogen target in the cell [29], showed that reactions with three particles in the final state, where two of them are charged, can be identified provided that the shape of background from the walls is known experimentally. Now, as was demonstrated above, we can assume that for both proton and deuteron beams we can reconstruct the interaction point in the long target. The track

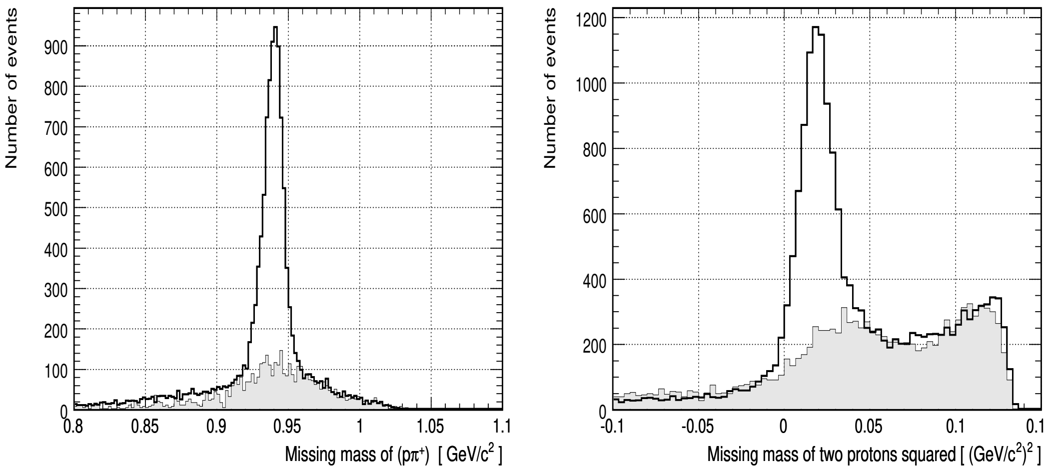

Figure 8: Missing–mass distribution for the reactions $pp \to p\pi^+X$ (left panel) and $pp \to ppX$ measured with the $(20 \times 20 \times 380\ \mathrm{mm}^3)$ storage cell and the 831 MeV proton beam. The open histograms represent the results obtained with the hydrogen gas while the shaded areas show the 'background' contributions measured with nitrogen in the cell. These latter distributions have been normalised to the hydrogen data to the right of the peaks.

information from the forward detector for two fast charged particles, is sufficient to identify the $dp \to (pp)n$ reaction. In Fig. 9 the results of the MC simulation are presented for the deuteron charge–exchange breakup reaction for a 4 mm horizontal wide beam. The left panel shows the reconstructed missing mass spectra *versus* the vertex z coordinate in the cell target, while on the right the expected missing–mass distribution of the $p(d, 2p)X$ reaction is shown. This spectrum reveals a well defined peak at the neutron mass, with an rms value of about $14\,\mathrm{MeV/c}^2$, and this could be clearly separated from the pion production which starts above $1.1\,\mathrm{GeV/c}^2$. However, the peak degrades significantly if the width of the beam is increased to 8 or 12 mm.

5.1.5 Missing–mass distributions for $dp \to p_{\mathrm{sp}}d\pi^\circ$

In the case of an incident deuteron, a *spectator* proton (p_{sp}) would have roughly half the momentum of the beam and be detectable over a range of angles, as shown in Fig. 6. As already stressed, $dp \to p_{\mathrm{sp}}d\pi^\circ$ events are confined to a small island in the $\Delta t_{\mathrm{tof}}(\vec{p_1}, \vec{p_2})$ plot of Fig. 7. The identification can be confirmed by looking at the missing mass distribution, which is shown in Fig. 10. The π^0 peak is evident for both short and long targets, though the width is broader in the case of the cell. However, even this is sufficient to separate single– from double–pion production.

5.1.6 Identification of pp (dp) elastic scattering with a long target

The experience gained during the PIT commissioning run [29], confirmed our suspicion that the detection of only a single track in the forward detector would not allow us to identify clearly elastic scattering on hydrogen. The missing–mass spectra of Fig. 11 were deduced from such single–proton events in the forward detector system. One cannot distinguish the signal (H_2 target) from the 'background' (N_2 target), because the distributions

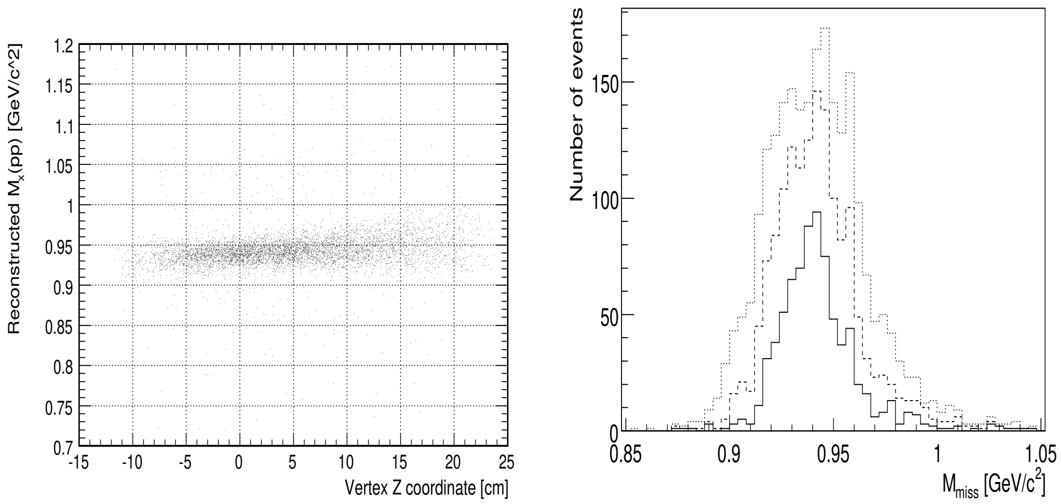

Figure 9: Simulation of the $p(d, 2p)X$ reaction at $T_d = 1.2$ GeV with the long cell target, both final fast protons being detected in the FD. The left panel shows the variation of the $p(d, 2p)X$ missing mass along the target length whereas the right panel sums all events. The horizontal width of the COSY beam was assumed to be 4 mm (solid histogram). The resolution gets poorer for wider beams, as can be seen from the simulations given in the right panel for 8 mm (dashed) and 12 mm (dotted) histograms, respectively.

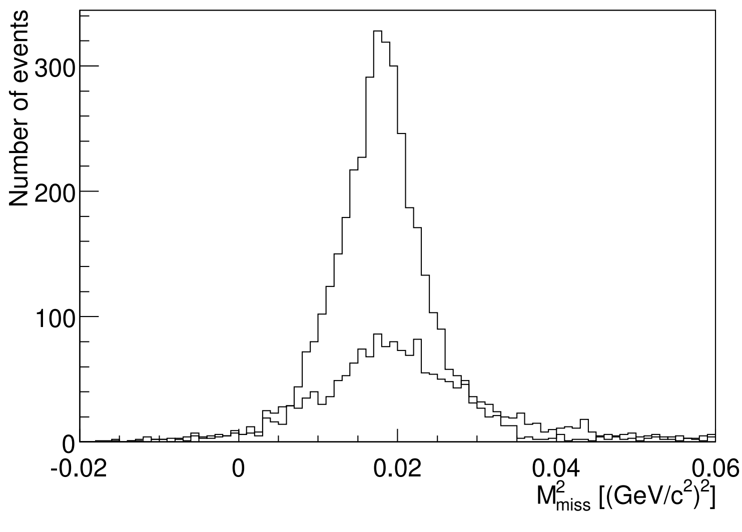

Figure 10: Missing–mass–squared for the $dp \to p_{sp}dX$ reaction obtained with a 'point–like' (higher histogram) and long (lower histogram) target.

have similar shapes with the same peak position. In order to identify dp elastic reaction with the PIT at ANKE it is crucial to have the STT system installed for the detection of recoil protons in coincidence with fast deuterons in the forward detector. The integration of the PIT with the STT system will be tested during the Jan/Feb 2007 beam time (see Exp.#159 [25]).

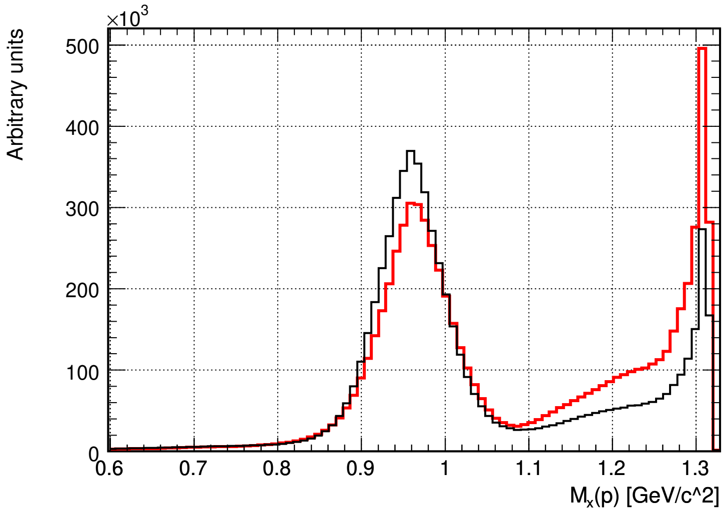

Figure 11: Single–arm missing mass spectra for 831 MeV protons scattered from a H_2 target (black) and N_2 target (red, lower histogram).

5.1.7 Background and resolution under PIT conditions

As discussed in the previous paragraph, in order to identify reactions with at least two charged particles in the final state, it is crucial to know the shape of the background under any missing–mass peak originating from production on the cell walls. The experience that we gained during the commissioning runs with the proton beam and hydrogen target cell, proved that this is in principle possible and could be tested with nitrogen gas in the cell.

With a deuteron beam, and hence with different nuclear reactions, it is difficult to predict the exact shape of the background from the cell walls under experimental conditions. One of the important points is how well the COSY beam can be prepared (cooled *etc.*) to pass through the long cell without touching the walls. This we will know only after the first pilot measurements have taken place at the beginning of 2007. At the present moment we can only assume (without proof) that this is possible, as already demonstrated for the proton beam.

In order to know the resolution under PIT conditions, a simulation has been performed that takes into account the thickness of the cell material and the density distribution along the extended target. As an example, Fig. 12 shows the resolution in excitation energy of the two protons from the charge–exchange breakup reaction with an extended target. The results, $\sigma(E_{pp}) \approx 0.2 - 0.4\,\text{MeV}$ are only slightly poorer than the analogous figures obtained with the cluster target, $\sigma(E_{pp}) \approx 0.1 - 0.3\,\text{MeV}$ for the energy range of interest $E_{pp} < 3\,\text{MeV}$. The missing–mass resolution for the neutron (Fig. 9) and π^0 (Fig. 10) also do not differ very much from the ones obtained with the cluster ('point like') target [3].

6 By–products of the investigation

In order to identify the reaction vertex and also control the background when working with a long target cell, it is necessary to measure two charged particles either in the FD or the STT. Even with this restriction, data on several other reactions will be taken simultaneously. Since these are not to be taken as primary motivations for this proposal,

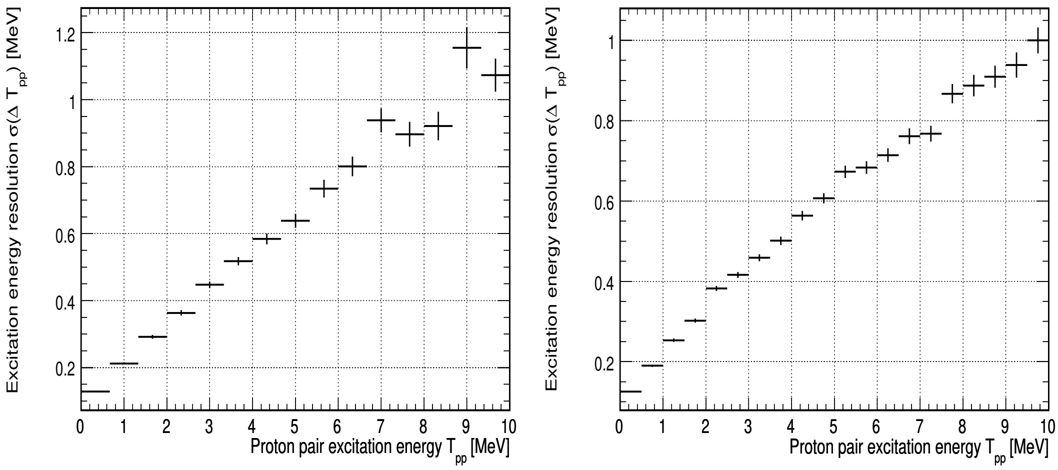

Figure 12: Simulation results for the excitation energy resolution in the CE breakup reaction with a long target for two different deuteron beam energies: T_d=1.2 GeV (left panel) and T_d=2.23 GeV (right panel).

they are here only indicated briefly to show that they have been thought about!

6.1 Single–meson production

The quasi–free $np \to d\pi^0$ reaction is obtained from the study of $dp \to dp_{\rm sp}\pi^0$ events, where the final proton is essentially a spectator whose only influence is through the smearing of the kinematics. However, data away from the spectator region are also of interest for the study of pion production more generally. The theory of this particular process at low dp excitation energies is very close to that of $dp \to {}^3\mathrm{He}\,\pi^0$ [32]. Although the reaction might also be thought of as exciting $I = \frac{1}{2}$ nucleon isobars, such as the Roper resonance, through $\vec{d}\vec{p} \to dN^*$, in our energy domain it is more likely that the reaction proceeds dominantly through the excitation of the Δ inside the projectile deuteron.

6.2 $\vec{d}\vec{p} \to p_{\rm sp} d(\pi\pi)^\circ$

The threshold for quasi–free $np \to d(\pi\pi)^\circ$ is at about 580 MeV, which means that the reaction could be studied well for a deuteron beam energy of 1.6 GeV, though the overall phase space at 1.2 GeV would be limited. The major interest here is in the study of s–wave pion pairs and the ABC phenomenon under clean conditions with polarised beam and target. Data on two–pion final states in $\pi^- p$ [33], pp [34], and pd [35] collisions all show interesting effects when the overall excitation energy is less than 100 MeV.

6.3 $\vec{d}\vec{p} \to \{pp\}\Delta^0$

The charge exchange of 2 GeV deuterons leading to a final Δ^0 isobar rather than a neutron was studied by the SPESIV collaboration. Such events will be present in the 1.6 GeV data set but the interpretation is more complicated than for the neutron final state because at such large momentum transfers the form factors of Eq. (6) become quite small.

6.4 $\vec{d}\vec{p} \to {}^3\mathrm{H}\,\pi^+$

For the cluster target some reactions were identified where only one charged particle emerged, as for example in $\vec{d}\vec{p} \to {}^3\mathrm{He}\,\pi^0$. This approach is no longer viable with the target cell but, as can be seen from Fig. 6, for certain kinematic ranges it should be possible to measure the ^{3}H and π^+ from the $\vec{d}\vec{p} \to {}^3\mathrm{H}\,\pi^+$ in coincidence. It should be noted that in the forward direction only two invariant amplitudes are needed to describe the reaction. Their magnitudes are fixed by the differential cross section and A_{yy} but a measurement of the spin–correlation parameter $C_{y,y}$ is needed to fix the relative phase [36].

6.5 $\vec{d}\vec{p} \to \{pp\}n$

It should be possible to measure the spin–correlation parameter $C_{y,y}$ in large momentum transfer charge–exchange, $\vec{d}\vec{p} \to \{pp\}n$ [37]. However, for both this and backward elastic scattering $\vec{d}\vec{p} \to pd$ the statistics will be limited.

7 Requested Beam Time

7.1 Expected luminosity

In order to estimate the required beam time for the proposed measurements, we assume a luminosity of $L = (2-3) \times 10^{29}\,\mathrm{s}^{-1}\mathrm{cm}^{-2}$ (with $\approx 1 \times 10^{10}$ stored polarised deuterons, $f_{\mathrm{rev}} = 1.6\,\mathrm{MHz}$, and $d_t = 1.5 \times 10^{13}\,\mathrm{cm}^{-2}$). It should be mentioned that with 3 day's cluster target measurements [3, 4] we had a luminosity of $L = 1 \times 10^{30}\,\mathrm{s}^{-1}\mathrm{cm}^{-2}$ (with $\approx 4 \times 10^9$ stored polarised deuterons, $f_{\mathrm{rev}} = 1.6\,\mathrm{MHz}$, and $d_t = 1.5 \times 10^{14}\,\mathrm{cm}^{-2}$), which is roughly a factor of four times larger than expected with polarised ABS cell–target [29]. The statistical accuracy we achieved in the previous polarisation measurements with cluster target was about 4%. In order to achieve an accuracy $\leq 10\%$ in the beam polarimetry determination with the cell target (including uncertainties from statistics and background subtraction arising from the cell wall), we need at least 4×3 days $\approx$ two weeks of beam–time for the measurements at one energy.

7.2 Request

- The **proposal requires a TOTAL of four weeks** to determine the vector $C_{y,y}(C_{x,x})$ and tensor $C_{yy,y}$ spin correlation coefficients at two energies $T_d = 1.2\,\mathrm{GeV}$ (or $1.6\,\mathrm{GeV}$ depending on the quality of the deuteron beam and its ability to pass through the cell without touching into the walls) and $T_d = 2.23\,\mathrm{GeV}$.

- With the **PRESENT request** the collaboration asks for approval of **two weeks of beam time** to carry out the first measurements at $T_d = 1.2\,\mathrm{GeV}$.

References

[1] A. Kacharava, F. Rathmann, and C. Wilkin for the ANKE Collaboration, COSY Proposal #152, *Spin Physics from COSY to FAIR*, arXiv:nucl-ex:0511028.

[2] S. Yaschenko *et al.*, Phys. Rev. Lett. **94** (2005) 072304.

[3] D. Chiladze *et al.*, Phys. Lett. B **637** (2006) 170.

[4] D. Chiladze *et al.*, Phys. Rev. ST Accel. Beams, **9** (2006) 050101.

[5] A. Kacharava and F. Rathmann for the ANKE Collaboration, COSY Proposal #125, available from http://www.fz-juelich.de/ikp/anke/proposals.shtml.

[6] J. Bystricky *et al.*, Nucl. Phys. A **444** (1985) 597.

[7] R.A. Arndt *et al.*, Phys. Rev. C **62** (2000) 034005.

[8] M. Altmeier *et al.*, Phys. Rev. Lett. **85** (2000) 1819.

[9] R.A. Arndt *et al.*, Phys. Rev. C **50** (1994) 2731; C **56** (1997) 3005.

[10] A. de Lesquen *et al.*, Eur. Phys. J. C **11** (1999) 69.

[11] D.V. Bugg and C. Wilkin, Phys. Lett. B **152** (1985) 37.

[12] D.V. Bugg and C. Wilkin, Nucl. Phys. A **467** (1987) 575.

[13] G.G. Ohlsen, Rep. Prog. Phys. **35** (1972) 717.

[14] B. v.Przewoski *et al.*, arXiv:nucl-ex:0511028 (2003).

[15] J. Carbonell, M.B. Barbaro and C. Wilkin, Nucl. Phys. A **529** (1991) 653.

[16] M.B. Barbaro and C. Wilkin, J. Phys. G **15** (1989) L69.

[17] R.A. Arndt, W.J. Briscoe, R.L. Workman, and I.I. Strakovsky, http://gwdac.phys.gwu.edu/analysis/

[18] E. Aprile *et al.*, Nucl. Phys. A **379** (1982) 369; *idem* **415** (1984) 365.

[19] E. Winkelmann *et al.*, Phys. Rev. C **21** (1980) 2535.

[20] J. Arvieux *et al.*, Nucl. Instr. Meth. **A273**, 48 (1988).

[21] M. Haji-Said *et al.*, Phys. Rev. **C36**, 2010 (1987).

[22] S. Barsov *et al.*, Nucl. Instr. Meth. A **462** (2001) 364.

[23] R. Schleichert *et al.*, IEEE Trans. Nucl. Sci. **50**, 301 (2003).

[24] I. Lehmann *et al.*, Nucl. Instr. Meth. A **530**, 275 (2004).

[25] R. Schleichert for the ANKE Collaboration, COSY Proposal #159, (May 2006), available from http://www.fz-juelich.de/ikp/anke/proposals.shtml.

[26] F. Rathmann for the ANKE Collaboration, COSY Proposal #146, (May 2006), available from http://www.fz-juelich.de/ikp/anke/proposals.shtml.

[27] R. Engels *et al.*, Rev. Sci. Instr. **76** (2005) 053305; R. Engels *et al.*, 6$^{\text{th}}$ Int. Conf. on Nuclear Physics at Storage Rings, Jülich–Bonn, Germany, 2005. Eds. D. Chiladze, A. Kacharava, and H. Ströher, Matter and Materials 30 (FZ Jülich, 2005), p. 381.

[28] W. Haeberli, Ann. Rev. Nucl. Sci. **17** (1967) 373.

[29] L. Barion *et al.*, Status Report for experiment #146.1, (May 2006), available from http://www.fz-juelich.de/ikp/anke/proposals.shtml.

[30] R. Engels *et al.*, Rev. Sci. Instr. **74** (2003) 4607.

[31] W. Haeberli *et al.*, Phys. Rev. C **55** (1997) 597; F. Rathmann *et al.*, Phys. Rev. C **58** (1998) 658, H.O. Meyer *et al.*, Phys. Rev. C **63** (2001) 064002.

[32] A. Boudard, G. Fäldt, and C. Wilkin, Phys. Lett. B **389** (1996) 440.

[33] S. Prakhov *et al.*, Phys. Rev. C **69** (2004) 045202.

[34] W. Brodowski *et al.*, Phys. Lett. B **550** (2002) 147.

[35] A. Abashian *et al.*, Phys. Rev. **132** (1963) 2296; M. Bashkanov *et al.*, Phys. Lett. B **637** (2006) 223.

[36] J.-F. Germond and C. Wilkin, J. Phys. G **16** (1990) 381.

[37] Yu.N. Uzikov, J. Phys. G **28** (2002) 13.